Journal of Solid State Chemistry **162,** 204–213 (2001)
doi:10.1006/jssc.2001.9248, available online at http://www.idealibrary.com on IDEAL®

Synthesis, Crystal Structures, and Properties of Edge-Sharing Tetrahedra Centered with Silicon and Cobalt: Cs_2CoSiO_4 and Cs_5CoSiO_6

Jens Hansing and Angela Möller[1]

Institut für Anorganische Chemie, Universität zu Köln, Greinstraße 6, 50939 Köln, Germany

Published online June 29, 2001

IN HONOR OF PROFESSOR PAUL HAGENMULLER ON THE OCCASION OF HIS 80TH BIRTHDAY

Cs_2CoSiO_4 and Cs_5CoSiO_6 were obtained from reactions of Cs_2O, CdO, and SiO_2 with cobalt plates in Ag containers which were encapsulated in glass ampoules under an Ar atmosphere. Cs_5CoSiO_6 is formed at 350°C (40 d) and Cs_2CoSiO_4 at 450°C (30 d) in an oxidation process under reduction of Cd^{2+} to the metal. Cs_2CoSiO_4 crystallizes in the space group $Cmc2_1$ (a = 582.5(1) pm, b = 1243.3(3) pm, c = 815.7(1) pm, R_{all} = 0.066) and Cs_5CoSiO_6 in $P2_1/n$ (a = 670.57(7) pm, b = 1080.8(2) pm, c = 1646.1(2) pm, β = 94.89(1)°, R_{all} = 0.052). Both compounds have the characteristic feature of edge-sharing tetrahedra centered with cobalt and silicon, forming dimers in common. Magnetic and luminescence measurements were carried out for Cs_2CoSiO_4, and UV–VIS–NIR–MIR–FIR spectra were recorded for both compounds. The electronic structures are described in terms of the angular overlap model.

Key Words: **crystal structure; silicate; cobalt; cesium; magnetism; spectroscopy.**

INTRODUCTION

Structural information about orthosilicates of transition metals, A_2MSiO_4 with A = Li–Cs, is still obtained mainly from X-ray powder diffraction data assuming isotypic structures. All known anhydrous silicates containing cobalt cations, e.g., Li_2CoSiO_4 (1), $Cs_2CoSi_5O_{12}$ (2), K_2CoSiO_4 (3), and $Na_2CoSi_4O_{10}$ (4), share the same structural feature of corner-sharing [SiO_4] and [CoO_x] polyhedra (x = 4, 6). Hofmann and Hoppe reported the first example of an edge-sharing arrangement of square-planar [NiO_4] with tetrahedral [SiO_4], $Rb_5LiNiSi_2O_8$ (5). Only recently, many examples have been synthesized and characterized by different physical measurements, e.g., $A_6MSi_2O_8$ and $A_4MSi_2O_7$ (A = K–Cs, M = Ni, Cu) (6). An interesting structure type for linking tetrahedra of different cations, e.g., Li^+ and M^{5+}, has been found for Cs_2LiMO_4 (M = As, Mn) (7). Cs_2CoSiO_4 is isotypic. The characteristic dimeric unit of edge-sharing tetrahedra has been observed, e.g., for $K_6Fe_2O_6$ (8) with typical metal–oxygen distances, $d(Fe^{3+}–O)$ = 185–195 pm. The interatomic distances for [SiO_4] tetrahedra are, of course, considerably shorter (≈163 pm), which reduces d(M–Si) drastically. Cs_5CoSiO_6 (9) can be regarded as a derivative of the above-mentioned structure when Fe^{3+} is substituted against Si^{4+} and Co^{3+}, respectively, and simultaneously eliminating one alkali metal cation. Apart from the crystal structures of these novel compounds, we report some of their physical properties.

EXPERIMENTAL DETAILS

Bright-blue single crystals of Cs_2CoSiO_4 and dark green ones of Cs_5CoSiO_6 were obtained under an inert gas atmosphere (Ar) by annealing intimate mixtures of "Cs_2CdO_2" (≡ $Cs_{14}Cd_9O_{16}$ (10)) (from Cs_2O and CdO) and SiO_2 in the presence of excess Cs_2O (typical molar ratio 1:1:2) between two cobalt metal plates in sealed Ag containers at 450°C (30 d) and 350°C (40 d), respectively. For protection, the containers were encapsulated in glass ampoules. The compounds are sensitive to moisture and, therefore, all preparations were carried out in a glovebox (Braun). Single-crystal X-ray diffraction data were collected on an IPDS diffractometer (Stoe & Cie). The program system X-RED/X-SHAPE was used for the numerical absorption correction (11). EDX analyses were carried out for both compounds on different crystals, confirming the composition. The reactivity of the system Cs–Co–Si–O–M with M = Ag, Cd was investigated by thermal analysis, DTA, on an STA-409 (Netzsch). The samples were sealed under an Ar atmosphere in self-made Ag containers fitted to a DSC sample holder. Absorption spectra were recorded at room temperature on CARY E05 (Varian) and IFS-v66-s (Bruker) instruments using selected crystals encapsulated in CsCl pellets and in

[1] To whom correspondence should be addressed. E-mail: angela.moeller@uni-koeln.de.

0022-4596/01 $35.00

PE (polyethylene) for the FIR spectra. Luminescence spectra (2 nm step width) of pure samples of Cs_2CoSiO_4, sealed in silica glass ampoules, were obtained at room temperature with a "triggered" (separated photodiode) Nd:YAG laser (Spectra Pysics, GCR 11, 355 nm, max. energy per pulse (9 ns): 20 mJ). A 0.27-m monochromator (Spectroscopy Instruments, SP-275M), a photomultiplier (Hamamatsu, R2949), and a photon counter (Stanford Research, SR400) were used for detection and recording. The magnetic behavior was measured on a Faraday magnetometer (field cooled, 1 Tesla). The sample was encapsulated under an Ar atmosphere in silica glass containers. The magnetic data have been corrected for diamagnetic contributions (12) resulting from the container material and the respective compound.

RESULTS AND DISCUSSION

Reactivity in the Systems: Cs–Co–Si–O–M with M = Ag, Cd

Two different orthosilicates with cesium and cobalt have been obtained via redox reactions at 350°C (Cs_5CoSiO_6) and 450°C (Cs_2CoSiO_4), respectively. This type of reaction has been used previously for synthesizing a wide variety of oxo-metallates (13). In principle the reactions follow the simple equations:

$$2Co + 3Cd^{2+} \rightarrow 2Co^{3+} + 3Cd \quad (350°C)$$

$$Co + Cd^{2+} \rightarrow Co^{2+} + Cd. \quad (450°C)$$

Three observations are remarkable:

(a) Unlike the rubidium system (Rb_2CdSiO_4 (14)), no precursor such as Cs_2CdSiO_4 was observed at lower temperatures.

(b) The first step of the redox reaction at 350°C gives Cs_5CoSiO_6, e.g., trivalent cobalt, and cadmium metal.

(c) The final product seems to be obtained through a redox reaction between Co^{3+} and metallic Co, according to

$$2Cs_5CoSiO_6 + Co + SiO_2 \rightarrow 3Cs_2CoSiO_4 + 2Cs_2O.$$

Thermal analysis was performed on ground powder samples of Cs_2O, SiO_2, Co (powder), and CdO in sealed Ag containers in the temperature range 25–600°C (rate: 10 K/min). A broad exothermal peak with a shoulder to low temperatures was observed at $\approx$350°C. No weight loss and no further thermal effects were detected. The product obtained from these experiments was always Cs_2CoSiO_4 and Cd metal.

Another oxidizing agent, $Cs_5AgSi_3O_9$ (15), with a decomposition temperature of $\approx$450°C was used to oxidize powdered Co metal. Again, only Cs_2CoSiO_4 and Ag metal were detected from this reaction ($T \approx 450$°C). It is interesting to note that under these conditions (heating rate: 10 K/min) only the cobalt(II) orthosilicate is obtained, which is obviously more stable than that obtained with the Jahn–Teller-active ion Co^{3+} in Cs_5CoSiO_6.

Crystal Structure of Cs_5CoSiO_6

For crystallographic data and details of the structure determination see Tables 1 and 2. The characteristic structural feature of Cs_5CoSiO_6 is a dimer formed by edge connection of $[CoO_4]$ and $[SiO_4]$ tetrahedra. Unfortunately, the structure refinement suggests a statistical occupation of each tetrahedral site. The $[MO_4]$ units are drastically distorted with a bridging angle O–*M*–O of only $\approx$80° for the Co site and 92° for the Si site, Table 3. In Fig. 1 the dimers are denoted with Co and Si instead of *M*1 and *M*2 according to the highest participation of each cation on the particular site, e.g., *M*1 = Co and *M*2 = Si. It must be stressed that the observed interatomic distances represent only the averaged structure derived from a fractional occupation of *M*1: $\frac{2}{3}$ (Co) and $\frac{1}{3}$ (Si) and vice versa for *M*2. Typical interatomic distances for edge-sharing dimers can be obtained for example from $K_6Fe_2O_6$ (8) with $d(Fe^{3+}–O) = 185–195$ pm and $A_6MSi_2O_8$ or $A_4CuSi_2O_7$ with $d(Si–O) = 160–167$ pm (5, 6). If one takes the occupational site factor into account, the following interatomic distances can be calculated for $[M1O_4]$ with $d(M1–O) = 181$ pm (calc.) and 184 pm (obs.) and $[M2O_4]$ with $d(M2–O) = 169$ pm (calc.) and 171 pm (obs.).

In the crystal structure of Cs_5CoSiO_6 five independent crystallographic sites are observed for cesium. Figure 2 illustrates the different coordination spheres of cesium with oxygen and the connection with crystallographically equal cesium atoms. Furthermore, the next coordinating atoms of the dimeric unit (Co, Si) are given as well. All $[CsO_x]$ polyhedra are different and present a wide range of unusual coordination spheres, although this is common in cesium-rich oxometallates. The $[CsO_x]$ polyhedra share corners or edges with cobalt and silicium. In the case of Cs1 and Cs3 triangular faces built of oxygen atoms connect Cs with each cation of a dimer. Each of these two cesium atoms form a network via corner-sharing arrangements of oxygen atoms with crystallographically equivalent ones. $[Cs5O_x]$ polyhedra are linked with each other via edges and form zig-zag chains along [100]. Cs4 has the very low C.N. 4 and is coordinated by oxygen atoms to form an edge-shared dimeric unit with its crystallographic equivalent. Cs2 is in that respect isolated. All cesium atoms connect with crystallographically different ones via oxygen atoms. All oxygen atoms have C.N. 6 in common. Apart from O3 and O6 all coordination spheres consist of one *M* (Si or Co) and five cesium atoms. Because O3 and O6 represent the bridging oxygen atoms within the dimer, they connect only to four

TABLE 1
Crystallographic Data for Cs_2CoSiO_4 and Cs_5CoSiO_6

	Cs_2CoSiO_4	Cs_5CoSiO_6
Crystal system	Orthorhombic	Monoclinic
Space group	$Cmc2_1$	$P2_1/n$
Temperature (K)	293	293
Lattice constants (pm) (IPDS data)	$a = 582.5(1)$	$a = 670.57(7)$
	$b = 1243.3(3)$	$b = 1080.8(2)$
	$c = 815.7(1)$	$c = 1646.1(2)$
		$\beta = 94.89(1)^\circ$
Formula units per unit cell	$Z = 4$	$Z = 4$
Diffractometer	Stoe IPDS	Stoe IPDS
Radiation (Mo $K\alpha$) (pm)	71.073 (graphite monochromator)	71.073 (graphite monochromator)
Range	$2\theta_{max} = 56^\circ$	$2\theta_{max} = 56^\circ$
	$-6 \le h \le 7, -16 \le k \le 14, -10 \le l \le 10$	$-8 \le h \le 7, -14 \le k \le 14, -21 \le l \le 21$
F (000)	732	1456
Absorption correction	Numerical (11)	Numerical (11)
Absorption coefficient (mm^{-1})	$\mu = 14.37$	$\mu = 15.72$
No. of measured reflections	3071	10,968
No. of unique reflections	754	2614
R_{int}	0.170	0.054
Structure determination	SHELXS-86; SHELXL-93 (16)	SHELXS-86; SHELXL-93 (16)
Refined parameters	47	120
Goodness-of-fit	0.874	0.976
$R1$ [$I_0 > 2\sigma(I)$]	0.053	0.032
$R1$/w$R2$ (all data)	0.066/0.128	0.052/0.064
Racemic twin component	0.3(1)	

cesium atoms and to the two centers, $M1$ and $M2$, of one dimer.

Crystal Structure of Cs_2CoSiO_4

Cs_2CoSiO_4 crystallizes isotypic with Cs_2LiMnO_4 (7) and not with K_2CoSiO_4 (3). For crystallographic data and details of the structure solution see Tables 1 and 4. The characteristic feature of the structure is the uncommon edge connection of two tetrahedra. These are linked via corners to form layers parallel to (101), Fig. 3. Cesium atoms are coordinated by six oxygen atoms in a distorted pentagonal-pyramidal arrangement, Fig. 4. Each crystallographically independent cesium atom is

TABLE 2
Atomic Parameters and Anisotropic and Equivalent Displacement Factors (in pm^2) for Cs_5CoSiO_6

Atom[a]	x	y	z	U_{11}	U_{22}	U_{33}	U_{23}	U_{13}	U_{12}	U_{eq}
Cs1	0.09940(9)	0.71167(4)	0.32238(3)	324(3)	174(2)	291(3)	19(2)	69(2)	−1(2)	260(1)
Cs2	0.82302(9)	0.71017(4)	0.10341(3)	296(4)	261(5)	356(3)	−100(2)	113(2)	−23(2)	299(1)
Cs3	0.93958(9)	0.01550(4)	0.22531(3)	282(3)	199(2)	228(2)	5(2)	15(2)	19(2)	237(1)
Cs4	0.7470(1)	0.10257(6)	0.00637(3)	588(5)	653(4)	222(3)	166(2)	−99(3)	−364(3)	495(2)
Cs5	0.28309(8)	0.54886(5)	0.06900(3)	239(3)	310(2)	210(2)	36(2)	27(2)	31(2)	253(1)
$M1$[b]	0.9019(2)	0.3651(1)	0.14347(7)	192(8)	175(6)	122(6)	−3(4)	15(5)	−22(4)	163(4)
$M2$[c]	0.5507(2)	0.1249(1)	0.80164(9)	196(11)	126(7)	146(8)	5(5)	37(6)	−11(6)	155(5)
O1	0.767(1)	0.1906(6)	0.8364(3)	471(48)	439(36)	218(30)	−17(24)	31(28)	−248(30)	376(16)
O2	0.4388(9)	0.0540(5)	0.8752(3)	334(40)	259(26)	210(26)	48(21)	−8(24)	−146(25)	270(13)
O3	0.388(1)	0.2227(5)	0.7453(5)	588(57)	160(28)	774(51)	−57(28)	325(41)	121(28)	492(20)
O4	0.031(1)	0.2967(6)	0.0702(4)	402(48)	576(41)	288(33)	−126(28)	41(29)	−66(32)	421(17)
O5	0.675(1)	0.4335(6)	0.1105(3)	373(44)	561(40)	184(29)	8(26)	−5(26)	141(31)	374(16)
O6	0.576(1)	0.0290(5)	0.7163(4)	711(58)	190(28)	404(36)	83(23)	303(34)	193(29)	421(19)

[a] All atoms on 4*e* sites. [b] Site occupation factors for $M1$: k(Co1) = 0.667(8), k(Si1) = 0.333(8). [c] Site occupation factors for $M2$: k(Co2) = 0.304(8), k(Si2) = 0.696(8).

TABLE 3
Interatomic Distances (in pm) and Angles (in deg) for Cs_5CoSiO_6[a]

Cs1–O1	302.3(6)	Cs2–O1	303.5(6)	Cs3–O3	287.2(6)	Cs5–O5	293.8(6)		
–O4	305.9(7)	–O3	305.6(7)	–O2	300.4(6)	–O5	299.8(6)		
–O6	312.9(5)	–O4	309.8(6)	–O5	300.5(6)	–O6	301.4(6)		
–O2	321.3(6)	–O2	313.2(6)	–O1	319.3(7)	–O4	320.6(7)		
–O5	327.3(7)	–O5	315.5(7)	–O6	334.1(8)	–O1	324.9(6)		
–O3	343.8(8)	–O6	353.3(7)	–O3	344.7(7)	–O4	341.4(7)		
–O6	363.7(7)								
Cs4–O2	290.6(5)	*M*1–O4	171.3(7)	*M*2–O2	166.6(5)				
–O2	293.7(5)	–O5	173.5(6)	–O1	167.4(6)				
–O4	296.7(7)	–O3	193.5(7)	–O3	172.9(7)				
–O1	297.0(6)	–O6	196.9(7)	–O6	176.5(6)				
O4–*M*1–O5	116.5(3)					O2–*M*2–O1	112.2(3)		
O4–*M*1–O3	117.5(3)					O2–*M*2–O3	111.7(3)		
O4–*M*1–O6	111.7(3)	*M*1–O3–*M*2	95.2(3)			O2–*M*2–O6	112.9(3)		
O5–*M*1–O3	112.1(3)	*M*1–O6–*M*2	92.9(2)			O1–*M*2–O3	114.4(3)		
O5–*M*1–O6	113.7(3)					O1–*M*2–O6	112.4(4)		
O3–*M*1–O6	80.0(3)					O3–*M*2–O6	91.8(3)		

[a] M = Co and Si; see site occupation factors in Table 2.

connected via corners built of oxygen atoms to their equivalents forming layers perpendicular to the *b* axis. [$Cs1O_6$] and [$Cs2O_6$] polyhedra share common corners and edges. O1 is coordinated by one silicon and cobalt as well as two cesium atoms. The polyhedron can be described as a flattened tetrahedron. The other oxygen atoms have C.N. 6. These distorted polyhedra are built of four cesium atoms, one cobalt atom, and one silicon atom with the latter ones in a cis arrangement. For interatomic distances and selected angles see Table 5. Although silicon is coordinated by four oxygen atoms almost in an ideal tetrahedral way, this is not the case for the [CoO_4] unit with two sets of interatomic distances (194 pm and 206 pm) and one angle $\angle$(O3–Co–O2) = 76°. The latter one results from the edge connection with [SiO_4]. In Cs_2LiMnO_4 (7) one angle, $\angle$(O–Li–O) = 82°, and distances of d(Li–O) = 192 pm and 202 pm are observed. This is very similar to the [CoO_4] unit in Cs_2CoSiO_4. Si^{4+} accommodates the same site as Mn^{5+}, although they differ in terms of the interatomic distances, e.g., d(Mn–O) = 170 pm and d(Si–O) = 162 pm.

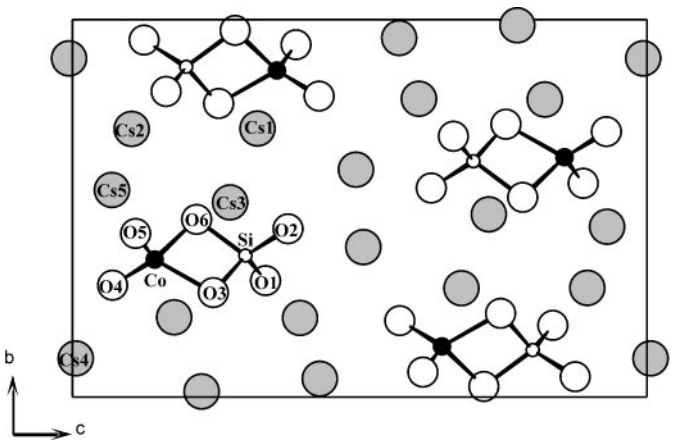

FIG. 1. Projection of the crystal structure of Cs_5CoSiO_6.

Absorption Spectrum of Cs_5CoSiO_6

The absorption spectrum of Cs_5CoSiO_6 is presented in Fig. 5. Tetrahedral cobalt(III) complexes are rare because they are rather unstable as a result of their electron configuration. Furthermore, a Jahn–Teller effect can be expected for $[CoO_4]^{5-}$ with a certain degree of distortion. The usual coordination for Co^{3+} is an octahedron and numerous examples are known.

Hagenmuller *et al.* (17) published absorption spectra of α-$KCoO_2$ containing the $[CoO_4]^{5-}$ chromophore. They discussed the unstable tetrahedral coordination of Co^{3+} in terms of a disproportionation according to $Co^{3+} \leftrightarrow Co^{2+} + Co^{4+}$, which has been proven to some extent by Mössbauer experiments for $LaCoO_3$ (18). This should give the superimposed absorption spectrum of both chromophores. A possible charge transfer corresponding to the gap between the valence and the conduction band (0.8 eV $\approx$ 6500 cm^{-1}) is suggested as well. In contrast to $KCoO_2$ the $[CoO_4]^{5-}$ complexes are isolated from each other in Cs_5CoSiO_6, so that it should be possible to obtain an absorption spectrum corresponding to the $[CoO_4]^{5-}$ chromophore. Still a statistical possibility of a small number of dimers containing Co^{3+} and Co^{4+} instead of Si^{4+} exists,

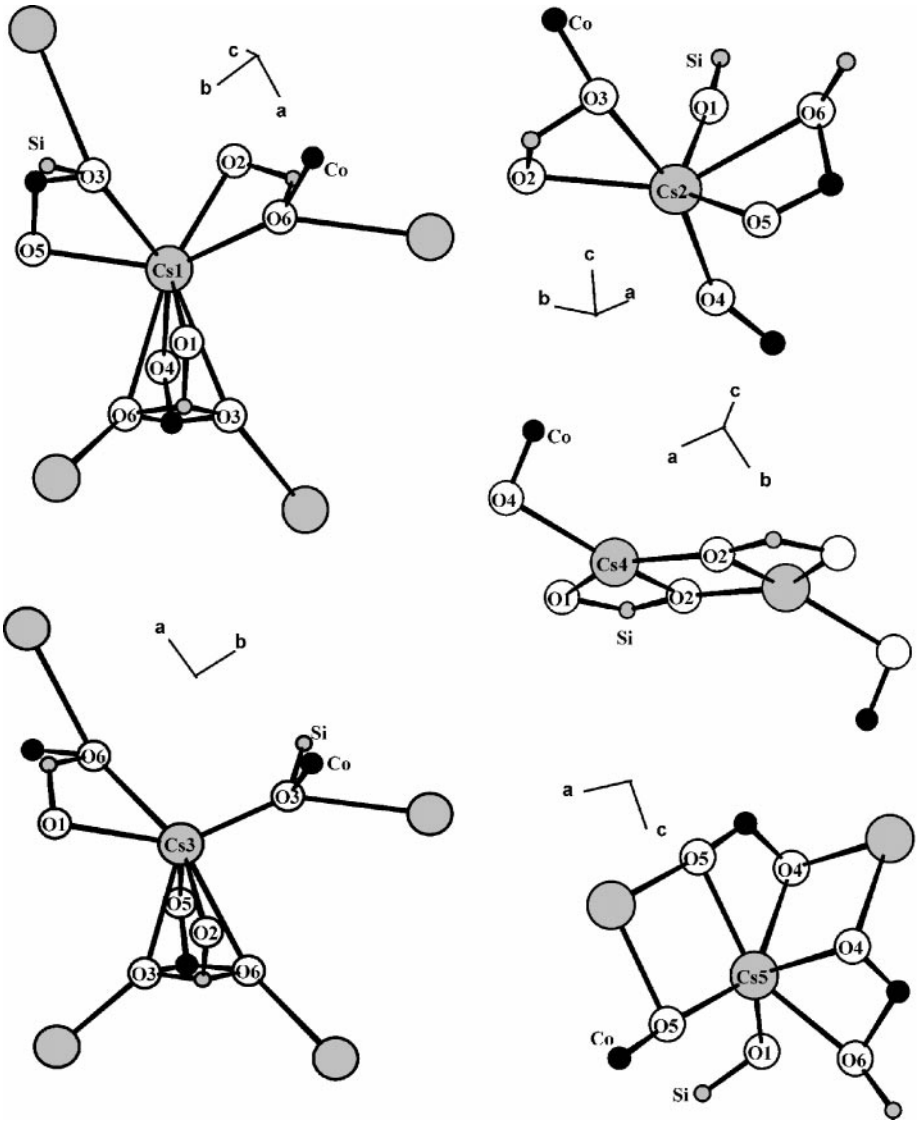

FIG. 2. Coordination spheres of $[CsO_x]$ polyhedra in Cs_5CoSiO_6.

which could lead to intervalence charge transfer processes in the visible part of the spectrum and/or a broad transition for $[CoO_4]^{4-}$ at about 16,000 cm^{-1} (17, 19). This might be the case for the absorption commencing at 10,000 cm^{-1}. The observed spectrum (Fig. 5) is similar to that reported for $KCoO_2$ (17).

TABLE 4
Atomic Parameters and Anisotropic and Equivalent Displacement Factors (in pm^2) for Cs_2CoSiO_4

Atom	Site	x	y	z	U_{11}	U_{22}	U_{33}	U_{23}	U_{13}	U_{12}	U_{eq}
Cs1	4*a*	0.5	0.0915(1)	0.5799(1)	262(10)	261(8)	249(10)	24(7)	0	0	258(5)
Cs2	4*a*	0	0.0739(1)	0.2302(2)	248(10)	291(9)	246(11)	−19(7)	0	0	262(5)
Co	4*a*	0.5	0.2935(3)	0.3079(5)	197(20)	186(16)	197(16)	−15(13)	0	0	194(8)
Si	4*a*	0.5	0.1977(6)	0.0205(9)	176(39)	233(37)	162(35)	27(26)	0	0	190(15)
O1	8*b*	0.275(2)	0.1585(9)	0.920(2)	332(75)	266(65)	260(72)	−2(50)	−2(55)	−53(59)	286(30)
O2	4*a*	0.5	0.327(1)	0.058(2)	320(89)	167(74)	4(65)	−25(59)	0	0	164(33)
O3	4*a*	0.5	0.146(1)	0.120(2)	199(93)	345(97)	46(85)	−125(62)	0	0	197(39)

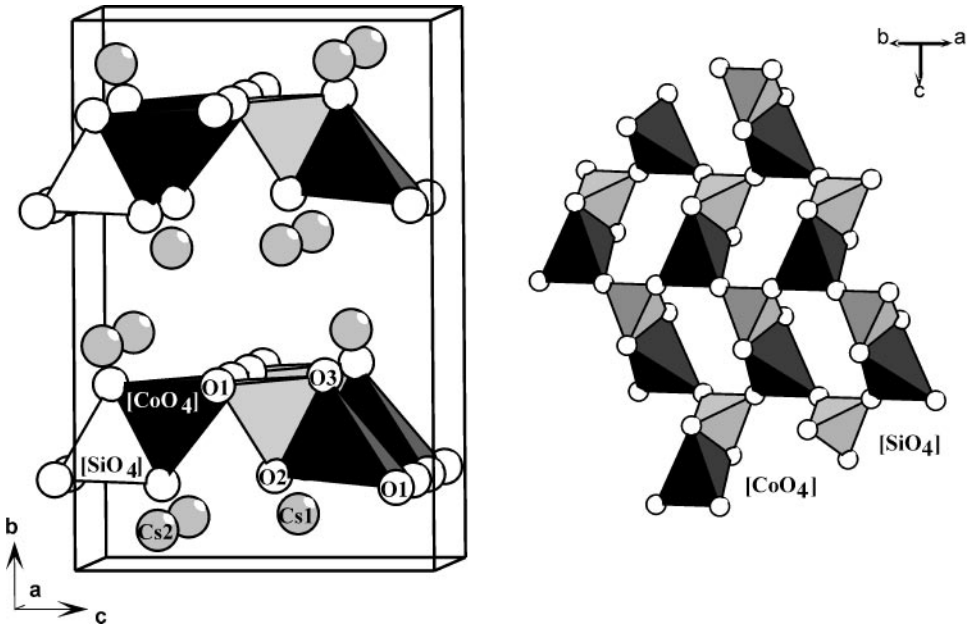

FIG. 3. Perspective view of the crystal structure of Cs_2CoSiO_4 (left) and an illustration of the connection between $[CoO_4]$ and $[SiO_4]$ tetrahedra forming layers (right).

Although a $[CoO_4]^{5-}$ complex should be unstable, there is still a possibility of stabilization to a certain extent via distortion (Jahn–Teller effect). A deviation from ideal tetrahedral symmetry is present in Cs_5CoSiO_6, because of the edge-sharing arrangement with $[SiO_4]$ units, e.g., $\angle$(O–Co–O) = 80°, all other angles approximately 115°, and two sets of interatomic distances (d(Co–O) $\approx$ 182 pm, 196 pm, see also (8)). Calculations within the angular overlap model (AOM) (20), using the computer program CAMMAG (21), have been carried out to obtain the transition energies for such a complex. The antibonding parameters, e_σ and e_π, represent the σ- and π-antibonding interactions in the complex. In Fig. 5 the parent terms are given for a symmetry reduction from T_d to D_{2d} with equal metal–ligand distances (189 pm) and a distortion for D_{2d} including $\angle$(O–Co–O) = 80° twice. The cases A and B (C_{2v}) represent the distortion of $[CoO_4]^{5-}$ present in Cs_5CoSiO_4. They differ only in the antibonding parameters used for the calculation. For A the antibonding parameters for each ligand were assumed to be equal (averaged environment) and for B they were fitted according to the interatomic distances, d(Co–O), mentioned above and see Table 6. Only the spin-allowed transitions belonging to the ^5D term of the free ion in a tetrahedral ligand field are included in Fig. 5 and Table 7. The transition energies produced by calculation B are in resonable agreement with the observed spectrum. Even the splitting of the ground state is illustrated and in agreement with the theoretical approach. Spin-forbidden transitions commence from 9000 cm^{-1} and might contribute to the unstructured absorption in the visible part of the spectrum. A superposition of the three chromophores $[CoO_4]^{n-}$ with $n = 4$, 5, 6 cannot be ruled out. The relative intensities of the absorption bands in the NIR and VIS, respectively, are very different from the spectrum of Cs_2CoSiO_4 (Fig. 5). For $KCoO_2$ a splitting of the band at $\approx$ 6300 and $\approx$ 8000 cm^{-1} is reported (17). This is very similar to what has been observed for Cs_5CoSiO_6.

To compare these results with other complexes one can relate the antibonding parameters to the tetrahedral splitting, $\Delta_t = -4/9\Delta_o$ and $\Delta_o = (3e_\sigma - 4e_\pi)$ (22). This gives $\Delta_t \approx -6000\ cm^{-1}$ for Cs_5CoSiO_6. This is approximately 30% or about 1800 cm^{-1} larger than $\Delta_t(Li_6CoO_4) = -4200\ cm^{-1}$ (23) and 1500 cm^{-1} or 25% for $\Delta_t(Cs_2CoSiO_4) = -4500\ cm^{-1}$ (see below). The antibonding parameters increase with a shortening of the bond length by the power of $\approx$ 5 (24). Neglecting the valence change and considering only the interatomic distances, e.g., $d(Co^{3+}–O) = 189$ pm and $d(Co^{2+}–O) = 200$ pm, respectively, one would expect a rise of 29% in the tetrahedral splitting energy, Δ_t, which is in excellent agreement with the observation. Furthermore, it is interesting to compare these results with those for octahedral complexes. The theoretical octahedral splitting of a formal "$[MO_6]^{n-}$" chromophore gives in this case $\Delta_o(Co^{3+}) = 13{,}500\ cm^{-1}$, which is approximately 10% less than what has been observed for Li_2MnO_3 (d(Mn–O) = 194 pm) with $\Delta_o(Mn^{4+}) = 14{,}500\ cm^{-1}$ (25)

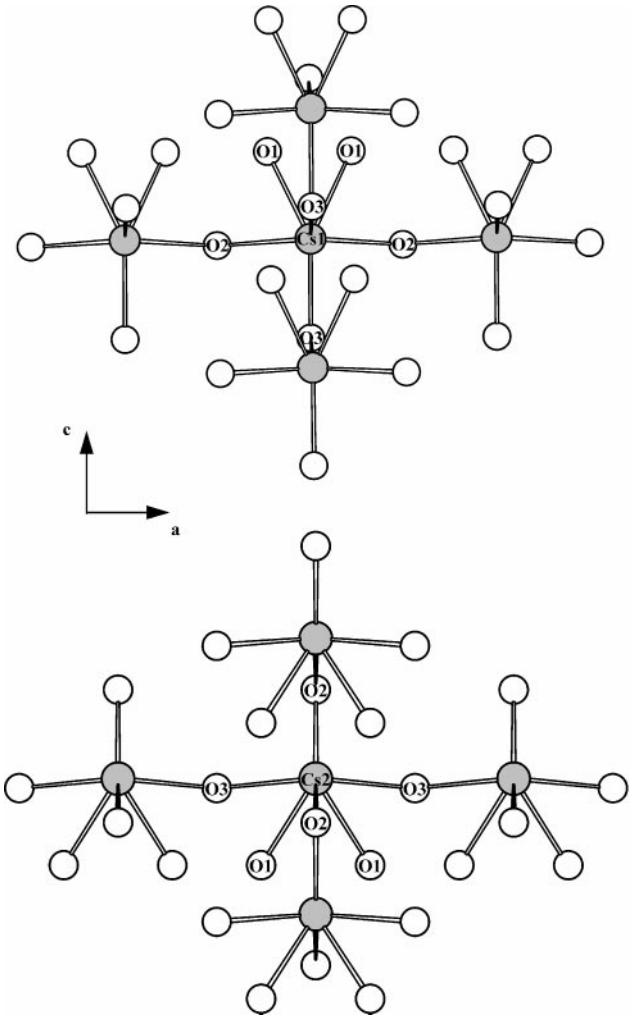

FIG. 4. Connection of [Cs1O_6] (above) and [Cs2O_6] (below) pentagonal pyramids to layers in Cs_2CoSiO_4.

and what can be estimated from the dependence on the interatomic metal–ligand distances and the change of the oxidation state.

Absorption and Luminescence Spectra of Cs_2CoSiO_4

The absorption spectrum of Cs_2CoSiO_4 with the parent terms and the calculated transition energies is illustrated in Fig. 5. In principle the same routine as described for Cs_5CoSiO_6 has been carried out with the interatomic distances $\bar{d}(Co^{2+}\text{–}O) = 199$ pm and the distortion angle 76° for D_{2d} according to the edge connection of the two tetrahedra centered by cobalt and silicon, respectively. The cases A and B (C_{2v}) represent the distortion found by X-ray crystal structure refinement and differ only in the set of antibonding parameters with respect to the differences in the bond length. Case A represents an averaged environment with equal sets of e_σ and e_π for each ligand. The antibonding parameters, e_σ and e_π, as well as the Racah parameters in terms of the AOM (20, 21) are given for case B in Table 6. Spin-forbidden transition energies have been calculated as well but have not been included in Fig. 5. The tetrahedral splitting can be derived from the e_σ and e_π values with $\Delta_t = -\frac{4}{9}\Delta_o = -\frac{4}{9}(3e_\sigma - 4e_\pi)$ (22) and yields $-4500\ cm^{-1}$ for Cs_2CoSiO_4. The larger value for $\Delta_t(Cs_2CoSiO_4)$ implies a more ionic bonding situation within the $[CoO_4]^{6-}$ complex than in Li_6CoO_4 ($-4200\ cm^{-1}$) (23) as a result of different alkaline cations and the silicate as well.

Luminescence measurements show an intense red emission $E_{max} = 12{,}900\ cm^{-1}$ with a half-width of $\approx 1350\ cm^{-1}$. This implies a Stokes shift of $\approx 2100\ cm^{-1}$ for the fluorescence from the lowest vibrational state of the excited state at $\approx 15{,}000\ cm^{-1}$ to various vibrational states of the electronic ground state. The interesting luminescence of Cs_2CoSiO_4 at room temperature obscures the investigation of the second-harmonic-generation (SHG) effect, which can be expected for acentric structures.

Magnetic Behavior of Cs_2CoSiO_4

AOM calculations with the program CAMMAG (21) were carried out in order to describe the magnetic behavior of Cs_2CoSiO_4 including contributions due to first- and

TABLE 5
Interatomic Distances (in pm) and Angles (in deg) for Cs_2CoSiO_4

Cs1–O2	309.0(5) (2×)	Cs2–O2	295(2)	O1–Co–O1	112(1)
–O3	311(2)	–O3	305.6(6) (2×)	O1–Co–O3	118.7(4) (2×)
–O3	317(1)	–O1	318(2) (2×)	O1–Co–O2	113.6(6) (2×)
–O1	318(2) (2×)	–O2	338(3)	O3–Co–O2	75.8(6)
Co–O1	194(1) (2×)	Si–O3	160(2)	O3–Si–O1	110.0(7) (2×)
–O3	204(2)	–O1	162(1) (2×)	O3–Si–O2	102.9(8)
–O2	208(2)	–O2	163(2)	O1–Si–O1	108(1)
				O1–Si–O2	113.0(6) (2×)
Co–O1–Si	144.5(8)	Co–O2–Si	89.4(8)	Co–O3–Si	91.9(9)

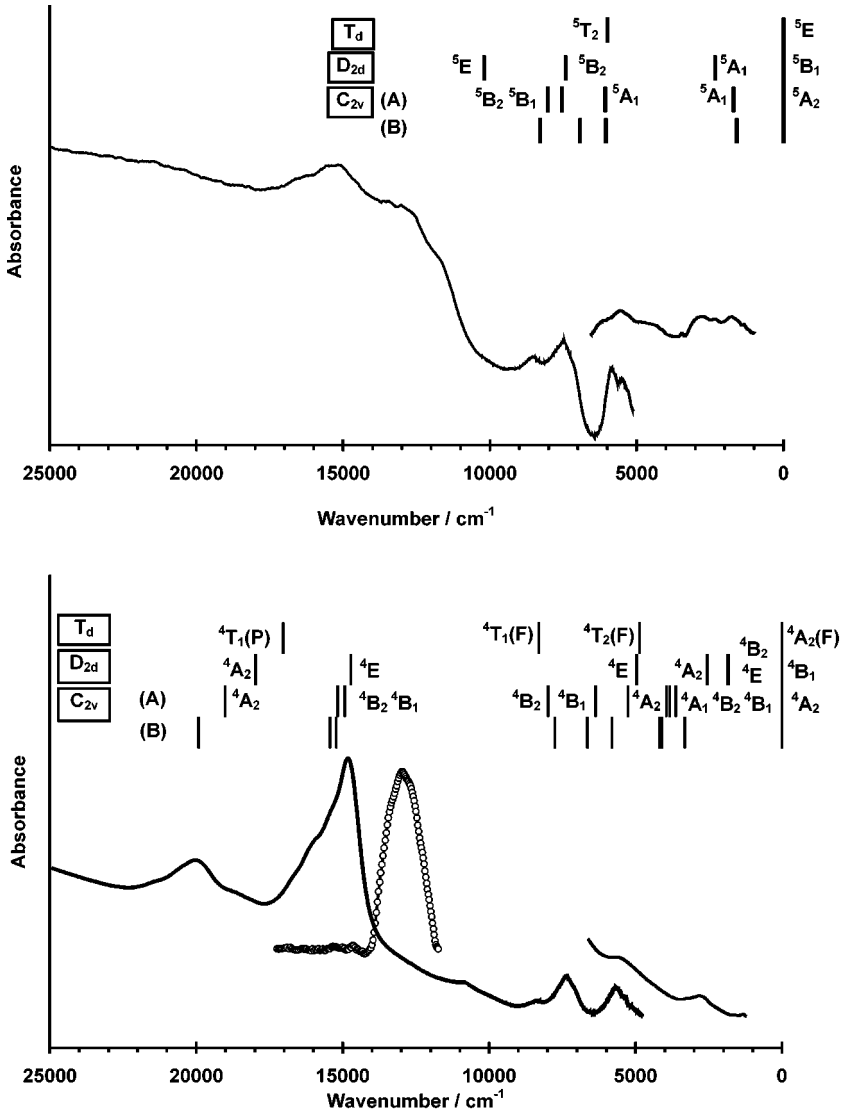

FIG. 5. Assignment and absorption spectra of Cs_5CoSiO_6 (above) and of Cs_2CoSiO_4 (below). The luminescence spectrum (○) for Cs_2CoSiO_4 is included as well.

second-order Zeeman effects. The data sets used for the input are those which have been derived via the calculation of band energies observed in the absorption spectrum. The spin–orbit coupling (ξ) and the orbital reduction (k) parameters (Table 6) were used to obtain a good agreement between calculation and the observed magnetic data. Since Cs_2CoSiO_4 follows the Curie–Weiss law with an antiferromagnetic interaction of $\Theta = -16$ K, the calculated data had to be adjusted to such a Θ value. Therefore, the calculated average susceptibilities were converted into the reciprocal ones, and then corrected to the temperature including the Weiss constant and then the molar susceptibilities and magnetic moments were recalculated. The experimental data for the magnetic moment illustrated in Fig. 6 drops from the ideal line at higher temperatures, which is probably an artifact of the measurement and not due to the properties of the sample. The overall agreement of observed and calculated data is good. The derived effective magnetic moment for Cs_2CoSiO_4, $\mu_{eff} = 4.2\ \mu_B$, is

TABLE 6
AOM Parameter (in cm^{-1}) for Cs_5CoSiO_6 and Cs_2CoSiO_4

	Cs_2CoSiO_4		Cs_5CoSiO_6	
	T_d, D_{2d}, C_{2v} (A)	C_{2v} (B)	T_d, D_{2d}, C_{2v} (A)	C_{2v} (B)
B	745	745		
C	2550	2550		
ξ	365	365		
k	0.7	0.7		
e_σ	6575	6150/7000	7725	7300/8000
e_π	2400	2300/2500	2425	2350/2500

TABLE 7
Observed and Calculated Transition Energies and IR Data (in cm^{-1}) for Cs_5CoSiO_6 and Cs_2CoSiO_4

Cs_2CoSiO_4			Co_2SiO_4 (26) (IR)		Cs_5CoSiO_6		
Observed	Calculated C_{2v} (B)	Observed (IR)			Observed (IR)	Observed	Calculated C_{2v} (B)
19800	19917	95			95	8500	8290
15500	15438	150			150	7300	6927
14900	15218	260	*260 (27, 28)*	G	260	5900	6050
7700	7756	290		G	290	2000	1591
6200	6645	360	392	v_2	360		
5750	5811	440//430			460//445		
4250	4184	485//510//560	484//513//575	v_4	485//510//560		
	4096	825	829	v_1	825		
3000	3323	855//905//960	875//973	v_3	850//910//960		

similar to $\mu_{eff}(Li_6CoO_4) = 4.1\ \mu_B$. The antiferromagnetic interaction in Li_6CoO_4 is smaller, $\Theta = -8$ K, and the effective spin–orbit coupling is about 45 cm^{-1} larger in Cs_2CoSiO_4.

IR Spectra of Cs_2CoSiO_4 and Cs_5CoSiO_6

The IR spectra of both compounds show the characteristic stretching modes for orthosilicates, Table 7 and Fig. 7. Tarte (26) published spectra of orthosilicates of the M_2SiO_4 type and the values obtained for the cobalt compound are included in Table 7 as well. In these compounds cobalt is coordinated by six oxygen atoms and the vibration modes are observed at lower wavenumbers than for the tetrahedrally coordinated cobalt in Cs_2CoSiO_4 and Cs_5CoSiO_6. For the $[CoO_4]$ units one can expect the v_3 and v_1 vibration mode at $\approx 450\ cm^{-1}$ as measured for ZnO (27). We observe shoulders in the prominent v_4(Si–O) mode centered at 485 cm^{-1} for Cs_2CoSiO_4 (I) at 440 cm^{-1} and for Cs_5CoSiO_6 (II) at 460 cm^{-1}. This shift can be expected from the shortening of the interatomic distance d(Co–O) and the difference in oxidation state. Lattice modes as reported for other orthosilicates and α-quartz (27, 28) are detected at 290 and 260 cm^{-1}. The bands below 200 cm^{-1} are tentatively assigned to Cs–O vibrations.

CONCLUSIONS

Both orthosilicates, Cs_2CoSiO_4 and Cs_5CoSiO_6, have the unexpected edge-sharing arrangement of two tetrahedra in common. Studies of the reactivity give evidence for the less stable configuration of high-spin trivalent cobalt in Cs_5CoSiO_6 and the further redox reaction yielding the more stable divalent cobalt compound, Cs_2CoSiO_4. The electronic structures of both compounds have been investigated by absorption spectroscopy. The results obtained for Cs_2CoSiO_4 suggest a higher tetrahedral splitting energy for the $[CoO_4]^{6-}$ chromophore than for Li_6CoO_4. The absorption spectrum of Cs_5CoSiO_6 gives some support for the presence of a high-spin $[CoO_4]^{5-}$ complex.

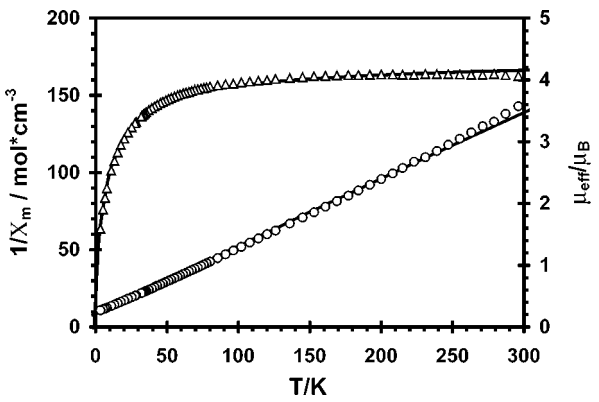

FIG. 6. Observed (△, ○) and calculated (—) magnetic data for Cs_2CoSiO_4.

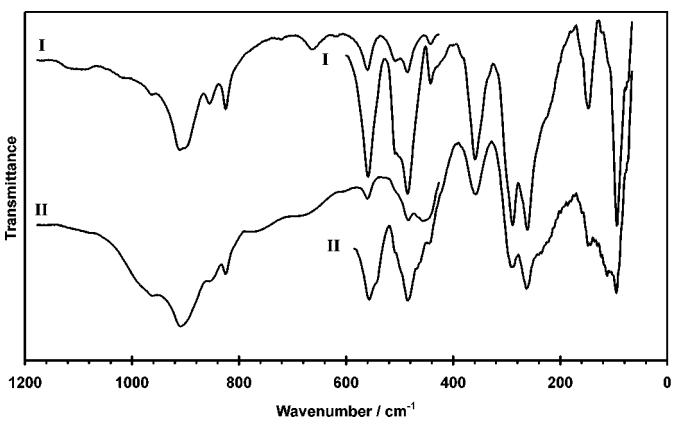

FIG. 7. Infrared spectra of Cs_2CoSiO_4 (I) and Cs_5CoSiO_6 (II).

ACKNOWLEDGMENTS

The authors are indebted to Dr. C. Wickleder for measuring the luminescence spectrum and the co-workers of Prof. R. Gross at the II. Physikalisches Institut, Universität zu Köln, for collection of the magnetic data and carrying out the EDX analysis. Financial support from the Deutsche Forschungsgemeinschaft, Bonn, is gratefully acknowledged.

REFERENCES

1. H. Yamaguchi, K. Akatsuka, M. Setoguchi, and Y. Takaki, *Acta Crystallogr.* **35,** 2680 (1979); *Acta Crystallogr.* **36,** 234 (1980).
2. A. M. T. Bell and C. M. B. Henderson, *Acta Crystallogr. C* **52,** 2132 (1996).
3. W. A. Dollase, *Powder Diffraction* **11,** 51 (1996).
4. G. Durand, S. Vilminot, M. Richard-Plouet, A. Derory, J. P. Lambour, and M. Drillon, *J. Solid State Chem.* **131,** 335 (1997).
5. R. Hofmann and R. Hoppe, *Z. Anorg. Allg. Chem.* **569,** 31 (1989).
6. A. Möller, *Z. Anorg. Allg. Chem.* **623,** 1685 (1997); A. Möller, *Z. Anorg. Allg. Chem.* **624,** 1085 (1998); A. Möller, *Z. Anorg. Allg. Chem.* **626,** 2251 (2000); J. Hansing, P. Amann, and A. Möller, *Z. Kristallogr. NCS* **216,** 17 (2001).
7. D. Fischer and R. Hoppe, *Z. Anorg. Allg. Chem.* **618,** 59 (1992).
8. H. Riek and R. Hoppe, *Angew. Chem.* **85,** 589 (1973); *Int. Ed.* **12,** 673 (1973); *Z. Anorg. Allg. Chem.* **408,** 151 (1974).
9. J. Hansing and A. Möller, *Z. Kristallogr.* **Suppl. 16,** 34 (1999).
10. E. Seipp and R. Hoppe, *Z. Anorg. Allg. Chem.* **549,** 119 (1987).
11. Stoe and Cie, X-SHAPE 1.01, X-RED 1.07, Darmstadt, 1996.
12. P. W. Selwood, "Magnetochemistry," 2nd ed., Interscience Publishers Inc., New York, 1956.
13. F. Bernhardt and R. Hoppe, *Z. Anorg. Allg. Chem.* **619,** 969 (1993); A. Möller and R. Hoppe, *Z. Anorg. Allg. Chem.* **620,** 581 (1994).
14. J. Hansing and A. Möller, *J. Solid State Chem.*, in press.
15. A. Möller and P. Amann, *Z. Anorg. Allg. Chem.* **627,** 172 (2001).
16. G. M. Sheldrick, SHELXS-86, SHELXL-93, Göttingen, Germany, 1986, 1993.
17. C. Delmas, C. Fouassier, and P. Hagenmuller, *J. Solid State Chem.* **13,** 165 (1975).
18. V. G. Bhide, D. S. Rajoria, G. R. Rao, and C. N. R. Rao, *Phys. Rev. B* **6,** 1021 (1972).
19. A. Möller, unpublished results for $[FeO_4]^{5-}$ (d^5) in A_5FeO_4, A = Li, Na, (K).
20. C. E. Schäffer and C. K. Jørgensen, *Mol. Phys.* **9,** 401 (1965) and references therein.
21. D. A. Cruse, J. E. Davis, M. Gerloch, J. H. Harding, D. J. Mackey, and R. F. McMeecking, CAMMAG, a FORTRAN computing package, University Chemical Laboratory, Cambridge, England, 1979.
22. A. Bencini, C. Benelli, and D. Gatteschi, *Coord. Chem. Rev.* **60,** 131 (1984).
23. A. Möller, *Chem. Mater.* **10,** 3196 (1998).
24. M. Bermejo and L. Pueyo, *J. Chem. Phys.* **78,** 854 (1983).
25. G. Meyer and R. Hoppe, *Z. Anorg. Allg. Chem.* **424,** 257 (1976).
26. P. Tarte, *Spectrochim. Acta* **19,** 25 (1963).
27. N. T. McDevitt and W. L. Baun, *Spectrochim. Acta* **20,** 799 (1964).
28. V. Hohler and E. Funck, *Z. Naturforsch.* **28b,** 125 (1973).